

A Critical Assessment of the Performance of Protein–Ligand Scoring Functions Based on NMR Chemical Shift Perturbations

Bing Wang,[†] Lance M. Westerhoff,[‡] and Kenneth M. Merz Jr.*[†]

Department of Chemistry, Quantum Theory Project, University of Florida, P.O. Box 118435 Gainesville, Florida 32611-8435, and QuantumBio Inc. 200 Innovation Boulevard, Suite 261, State College, Pennsylvania 16802

Received April 25, 2007

We have generated docking poses for the FKBP–GPI complex using eight docking programs, and compared their scoring functions with scoring based on NMR chemical shift perturbations (NMRScore). Because the chemical shift perturbation (CSP) is exquisitely sensitive on the orientation of the ligand inside the binding pocket, NMRScore offers an accurate and straightforward approach to score different poses. All scoring functions were inspected by their abilities to highly rank the native-like structures and separate them from decoy poses generated for a protein–ligand complex. The overall performance of NMRScore is much better than that of energy-based scoring functions associated with docking programs in both aspects. In summary, we find that the combination of docking programs with NMRScore results in an approach that can robustly determine the binding site structure for a protein–ligand complex, thereby providing a new tool facilitating the structure-based drug discovery process.

Introduction

The determination of the three-dimensional structures of protein–ligand complexes is the critical step in structure-based drug design. Recent technological advances in X-ray crystallography and NMR spectroscopy have dramatically increased the number of high-resolution structures of proteins and protein–ligand complexes. Despite their success, none of these two techniques are high-throughput enough to keep the pace of the discovery of new lead molecules and therapeutic targets in the postgenomic era. Therefore, surrogate (nonexperimental) approaches like molecular docking are used as virtual screening tools in the structure-based drug discovery workflow employed in the pharmaceutical and biotech industries.^{1–5} Interestingly, several NMR experimental approaches^{6,7} have been developed to determine the ligand binding mode without solving the 3D structure of protein–ligand complex by combining docking programs with NMR parameters such as saturation transfer difference (STD)⁸ and nuclear Overhauser effects (NOE).

Basically, molecular docking is used to generate poses that may or may not represent the best complementary match between two molecules: a receptor and a ligand. These poses are then scored using various scoring functions to predict which best represents the experimental or native conformation. The first step is a conformational sampling procedure, which can be performed using a genetic algorithm, Monte Carlo simulation, simulated annealing, distance geometry, and other miscellaneous methods.¹ The final docked conformations are selected based on a scoring function. In principle, the binding affinity from a rigorous free energy simulation is an ideal scoring function.^{9–12} However, it is not practical to use such a time-consuming approach in docking studies. Therefore, most current scoring functions are derived from force fields^{13,14} or empirical^{15–17} or knowledge-based potentials.^{18,19} Several comparative studies of various scoring functions have been reported.^{20–23} Unfortunately,

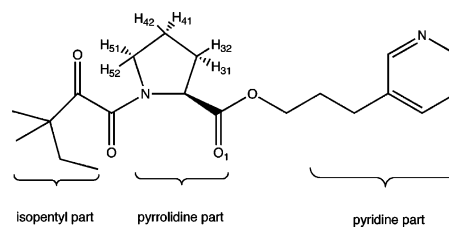


Figure 1. The chemical structure of GPI.

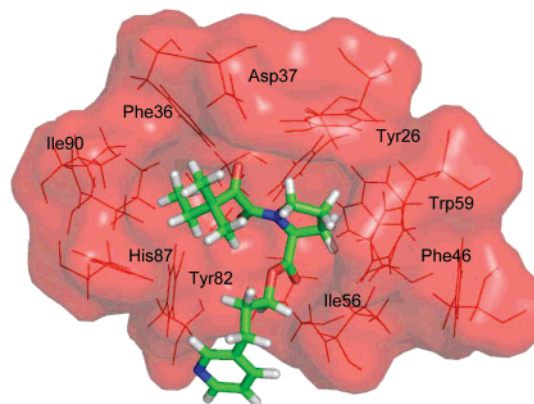


Figure 2. The binding site structure taken from NMR_6 (1F40).

the consensus is that energy-based functions are not accurate enough at this time to discriminate the native ligand structure from decoy sets, which often leads to multiple solutions for the best protein–ligand complex structure.^{2,3,5,23,24}

Recently, we have developed an accurate and fast approach to calculate NMR chemical shifts for biological systems using the divide-and-conquer method.²⁵ To our knowledge, this represents the first time that we calculate binding-induced chemical shift perturbations for an entire protein–ligand complex at the quantum mechanical level. We have previously applied this approach to the study the FKBP–GPI complex.²⁶ The GPI molecule (see Figure 1) is an effective inhibitor for the peptidyl-prolyl cis–trans isomerase (PPIase) activity of

* Author to whom correspondence should be addressed. E-mail: merz@qtp.ufl.edu.

[†] Department of Chemistry, Quantum Theory Project, University of Florida, P.O. Box 118435 Gainesville, FL 32611-8435

[‡] QuantumBio Inc. 200 Innovation Blvd, Suite 261, State College, PA, 16902

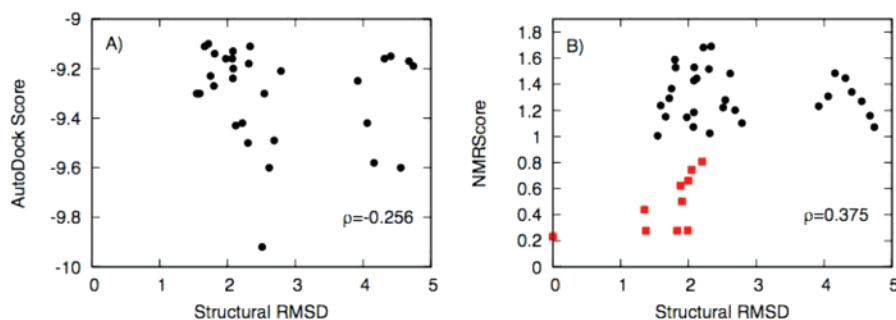


Figure 3. (A) AutoDock Score versus the structural RMSD (Å). (B) NMRScore versus the structural RMSD using the AutoDock derived poses. The red squares represent the experimental NMR ensemble structures of the GPI-FKBP complex.

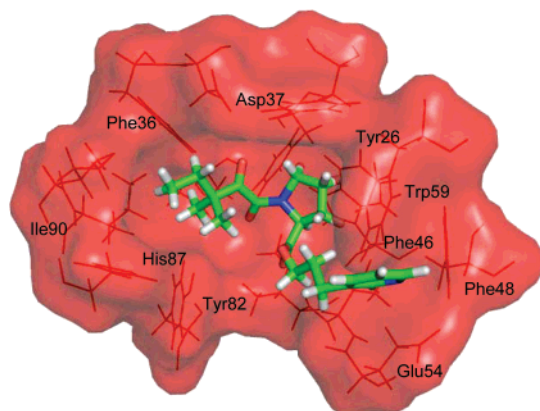


Figure 4. The binding site structure taken from Autodock_19, which shows the pyridine moiety of GPI is predicted to dock into a shallow groove formed by Phe46, Phe48, and Glu54.

FKBP. Ten NMR structures of this complex have been determined by Sich et al. (PDB code: 1F40).²⁷ An excellent agreement between experimental and calculated proton chemical shifts was obtained for the NMR models with Ile56–O1 (ligand) hydrogen bonds. Other models without this hydrogen bond tended to have much larger CSP root-mean-squared deviations (RMSD) between experiment and theory. This finding shows that this Ile56–O1 hydrogen bond is important for molecular recognition. Moreover, our approach was able to validate the binding site structure for the observed protein–ligand complex. Another application of our approach was to select the correct ligand structure from a set of decoy poses. Since CSP can be readily measured by NMR experiment with high precision, the RMSD between experimental and calculated CSP offers a straightforward manner to score different poses for a given protein–ligand complex. The major goal of this paper is to demonstrate that our approach, NMRScore, is able to improve the overall performance of scoring ligand poses in a protein binding pocket when compared to conventional scoring functions. To achieve this goal, we have docked the GPI molecule into the FKBP binding pocket using eight popular docking programs including AutoDock,¹³ Dock,¹⁴ eHiTs,²⁸ FlexX,²⁹ Fred,³⁰ Glide,^{31,32} LibDock,^{33,34} and MOE.³⁵ Then we compared the performance of the scoring function associated with each docking program with that of NMRScore. We would like to point out that the CSP information is not utilized during the process of NMR structure determination. Therefore, NMRScore is a fair scoring function for both NMR structures and docking poses.

Methods

Docking Procedure. A computational workflow specific to each of the docking/scoring functions was performed, leading to eight different populations of poses (one for each function). Before performing any scoring simulations, sets of ligand (GPI, see Figure 1) and enzyme (FKBP) input files were produced for each of the 10 NMR models in the NMR ensemble within the FKBP/GPI PDB file (1F40). Each of these input files included the fully protonated structures and experimentally determined coordinates originally found within 1F40. Atomic charges were assigned to each ligand atom using the Antechamber/DivCon application from the AMBER suite of programs,³⁶ and these charges were used for all score functions. Standard Cornell et al. *ff94*³⁷ atomic charges were assigned for FKBP. No preminimization or other cleanup was performed; hence, experimental coordinates were used throughout. Beginning with these standard input files, the eight docking/scoring studies summarized in Table 1 were performed (using both flexible ligand and rigid ligand docking) leading to eight different pose populations encompassing hundreds or thousands of different poses per function. In order to limit redundant poses within each population, the poses were clustered across the 10 NMR models using a 1.0 Å RMSD cutoff.

Scoring Procedure. Once the RMSD clustering was complete, the top 30 ranked poses for each program were used to calculate NMR chemical shift perturbations as implemented in the DivCon program.³⁸ We used the following specification to identify each docking pose: docking_program_number. The number is the ranking according to the corresponding scoring function in the docking program. For example, AutoDock_2 means the second ranked (i.e., second best predicted pose) structure generated by AutoDock. We computed the CSP RMSD from the experimental values to generate the value for NMRScore. The lower CSP RMSD, the better the NMRScore. To calculate the structural RMSD, we referenced every pose to NMR_6 (the sixth structural model from the 10 structure NMR ensemble) because it had the lowest CSP RMSD and we think it is the best NMR model for the “true” native structure (see Figure 2). For each docking program, we generated two figures summarizing the results: one is the program score versus structural RMSD, the other one is the NMRScore versus structural RMSD. We also include the NMRScore for the remaining experimental NMR structures of the FKBP–GPI complex from the NMR ensemble for reference in the latter figure. In addition, we showed the Spearman correlation coefficient ρ (see eq 1) for each scoring function and NMRScore against structural RMSD. A perfect scoring function only needs to provide the correct rankings of candidate molecules, no matter what the values of this scoring function. The Spearman correlation coefficient is a nonparametric measure of correlation and a proper quantitative measurement for this purpose since we observed very few “ties” in the scoring functions we tested.

$$\rho = 1 - \frac{6 \sum_{i=1}^n d_i^2}{n(n^2 - 1)} \quad (1)$$

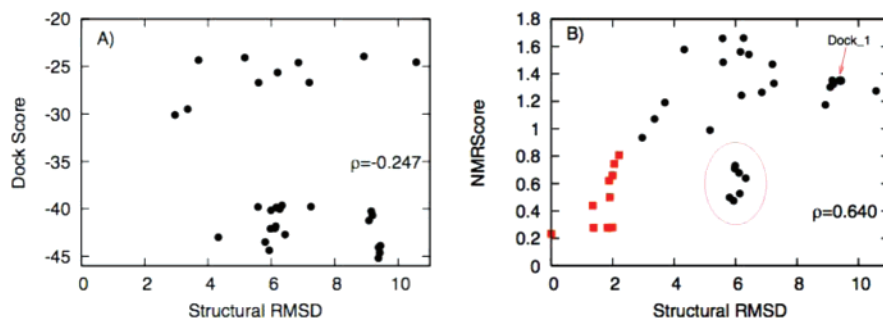


Figure 5. (A) Dock Score *versus* the structural RMSD. The rigid docking poses have scores above -30 whereas the flexible poses have scores below -40 . (B) NMRScore *versus* the structural RMSD using Dock derived poses. The red squares represent the experimental NMR ensemble structures of the GPI-FKBP complex.

Table 1. Summary of Docking/Scoring Protocols

program	flexible ligand	total poses	cluster RMSD, Å	final poses	notes
Autodock	yes	2560	1.0	30	in house, used standard settings
Dock (1)	yes	300	1.0	30	in house, used 20 atom flexibility and rigid docking
eHiTS	yes	500	1.0	30	in house, used -advanced keyword
FlexX	yes	250	1.0	30	in collaboration with BioSolveIT
Fred	yes	3000	1.0	30	in collaboration with OpenEye
Glide	no	285	1.0	30	in collaboration with J&J
LibDock	yes	5000	1.0	30	in collaboration with Pharmacoepia
MOE	yes	300	1.0	30	in collaboration with CCG

where d_i is the ranking difference of the i th pose between the structural RMSD and the scoring function (or NMRScore). N is number of pairs of values. In theory, ρ falls between -1 and $+1$, where $+1$ corresponds to a perfect correlation; -1 corresponds to a perfect inverse correlation, and zero corresponds to no correlation.

Results and Discussion

AutoDock. The 30 poses generated by AutoDock were clustered into two groups: one with a structural RMSD from

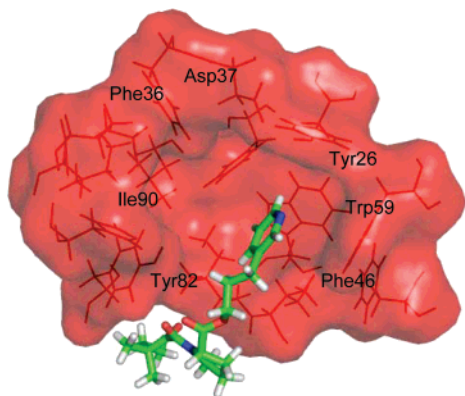


Figure 6. The binding site structure taken from Dock_1.

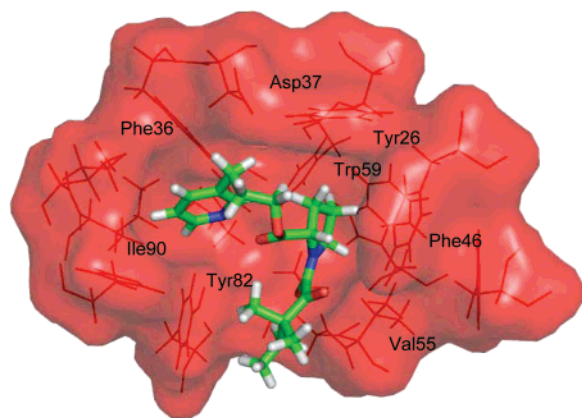


Figure 7. The binding site structure of Dock_3.

1.5 Å to 2.6 Å, the other from 3.9 Å to 4.7 Å (see Figure 3A). The pyridine moiety (see Figure 1) from the second RMSD grouping docks into a shallow groove formed by Phe46, Phe48, and Glu54, instead of the pocket formed by Ile56, Tyr82, and His87 as seen in the native structure (see Figure 4). The other regions of GPI are bound in a manner similar to that seen in the native structure. The AutoDock scoring function is based on a force field, which is typically not specifically developed for describing protein–ligand interactions. Therefore, it is not surprising that the Spearman correlation coefficient is negative for the AutoDock Score. NMRScore demonstrates that all of the “best” AutoDock poses (see Figure 3B) are not good models for the orientation of GPI in the FKBP binding pocket. We expect NMRScore to have an RMSD of below 1 ppm in order to indicate a good match with experiment. This is based on past experience with NMRScore on this system (see NMR structures in Figure 3A). None of the AutoDock structures reach this threshold, and as a result we would predict that AutoDock has not placed the ligand in a native-like configuration, which is, indeed, the case.

Dock. Two different settings of the Dock program were employed in order to utilize both flexible (20 atoms of GPI were flexible) and rigid ligand docking (for the results, see Figure 5). The range of structural RMSD for the docked poses was from 3 Å to 11 Å. Since there are several scoring functions available in the Dock program, we used the grid-based scoring function as a primary scoring function. According to this force field-based scoring function, the rigid docking poses have less favorable (more positive) Dock scores than the flexible docking poses (see Figure 5A). Dock_1 and Dock_2 placed the pyridine moiety into the major binding pocket (see Figure 6), resulting in a large structural RMSD (around 9.3 Å) and NMRScore (about 1.35 ppm).

Dock_3 and Dock_6 have the best NMRScore (CSP RMSD = 0.5 ppm) but have a different structure from the native one (structural RMSD = 6 Å). They are even better than some of the NMR ensemble structures in terms of NMRScore (see Figure 5B). This is because the pyridine and isopentyl parts of these structures swap their positions but the pyrrolidine moiety

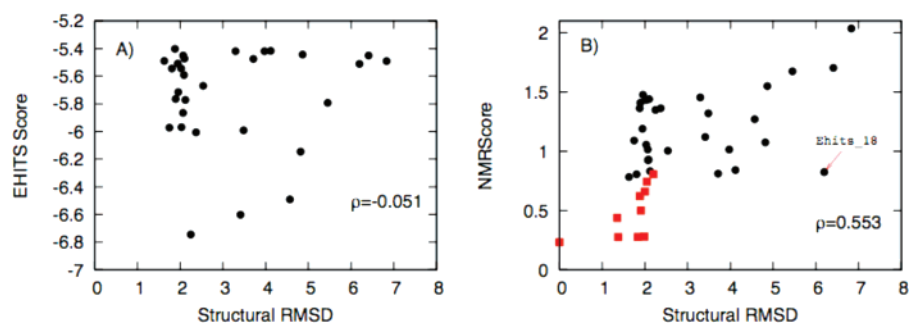


Figure 8. (A) EHITS Score vs the structural RMSD. (B) NMRScore versus the structural RMSD using EHITS derived poses. The red squares represent the experimental NMR ensemble structures of the GPI-FKBP complex.

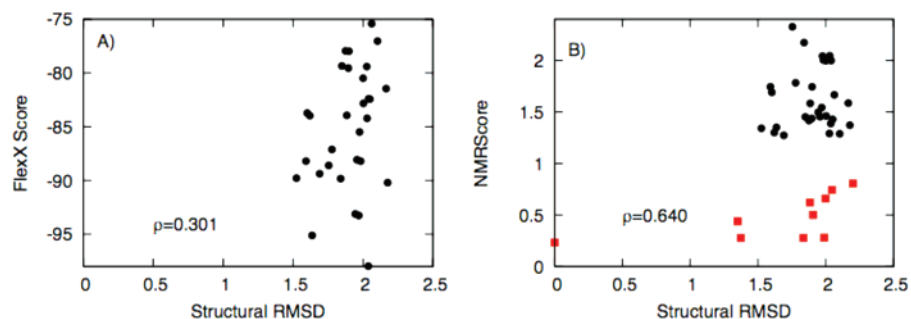


Figure 9. (A) FlexX Score vs the structural RMSD. (B) NMRScore versus the structural RMSD using FlexX poses. The red squares represent the experimental NMR ensemble structures of the GPI-FKBP complex.

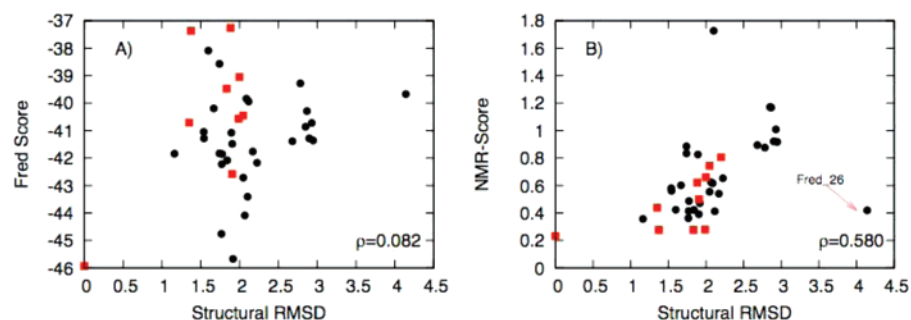


Figure 10. (A) Fred Score vs the structural RMSD. (B) NMRScore versus the structural RMSD using Fred poses. The red squares represent the experimental NMR ensemble structures of the GPI-FKBP complex.

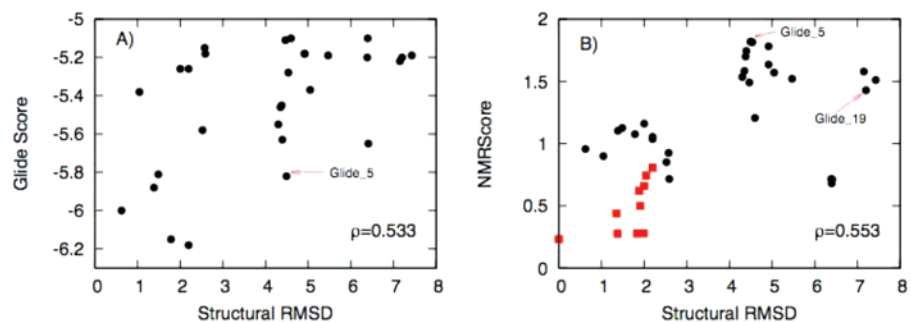


Figure 11. (A) Glide Score vs the structural RMSD. (B) NMRScore versus the structural RMSD using Glide poses. The red squares represent the experimental NMR ensemble structures of the GPI-FKBP complex.

remains at the central binding site (see Figures 1, 2, and 7). This orientation inside the binding site gives very large chemical shift perturbations for the protons in the five-membered ring because of the ring current effect, which is the major source of CSP for the GPI molecule upon binding with FKBP. Several other structures generated by the Dock program share similar features (see the cluster highlighted by a red oval in Figure 5B),

and it suggests that Dock has found an alternate solution to the structure of this complex. The pyridine ring in these poses could give large CSP for protons on Phe36 and Ile90, while that in the native structure would likely not. Therefore, inclusion of CSP from the side chains of the FKBP protein in NMRScore may differentiate these poses from the native structure. This problem can also be easily avoided by measuring NMR

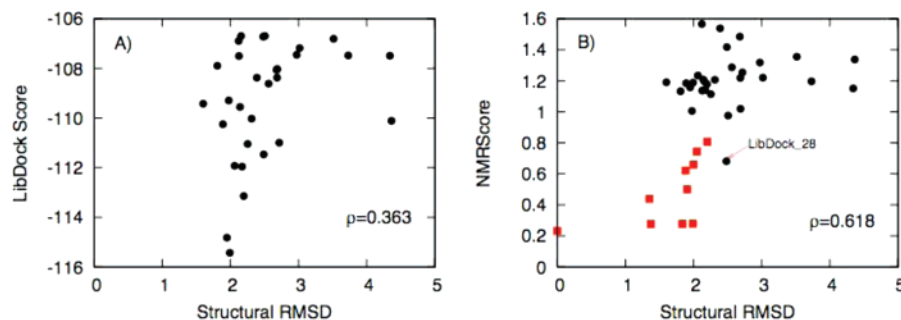


Figure 12. (A) LibDock Score vs the structural RMSD. (B) NMRScore versus the structural RMSD using LibDock poses. The red squares represent the experimental NMR ensemble structures of the GPI-FKBP complex.

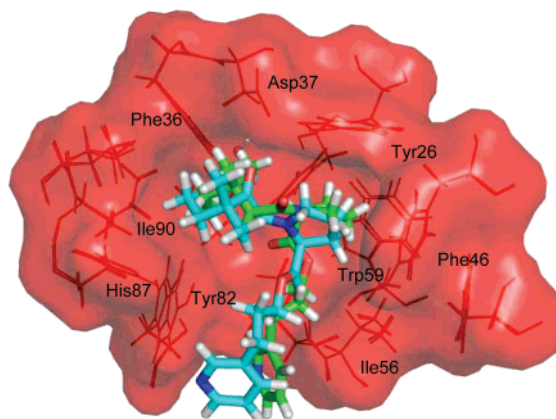


Figure 13. The binding site structure of LibDock_28 (green) and NMR_6 (cyan).

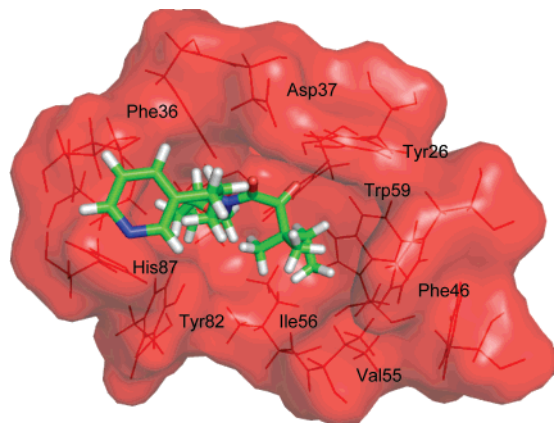


Figure 14. The binding site structure of MOE_1.

experimental NOEs between the ligand and the protein. Future studies will examine this interesting observation in more detail, but suffice it to say that NMRScore, in its current incarnation, would have provided two solutions for the FKBP–GPI complex. Nevertheless, the overall performance of NMRScore ($\rho = 0.64$) is much better than that of Dock Score ($\rho = -0.25$).

EHITS. The top 30 ranked poses by EHITS are spanned by a wide spectrum of structural RMSD from 1.6 Å to 7 Å (see Figure 8). The highest ranked pose (RMSD 2.2 Å) is close to the native pose of the FKBP–GPI complex when compared to other docked poses. However, many lower ranked poses also have relatively small structural RMSD (see Figure 8A). Therefore, it is difficult for EHITS scoring function to rank these native-like structures. Figure 8B plots NMRScore with respect to the structural RMSD for the top 30 poses. EHITS_21 has

the lowest NMRScore at 0.78 ppm and the lowest structural RMSD at 1.6 Å. The poses with larger structural RMSD tend to have the worst (larger values) NMRScore. One prominent exception is EHITS_18 that has a relatively low NMRScore (0.82 ppm) with a very different structure from the native one (RMSD 6.2 Å). Similar to Dock_3 and Dock_6 mentioned above (see Figures 6 and 7), the isopentyl and pyridine moieties of EHITS_18 switch their positions relative to the native structure, resulting in a large structural RMSD, whereas the pyrrolidine ring of EHITS_18 is kept inside the hydrophobic pocket formed by the side chains of Tyr26, Phe46, Trp59, and Phe99. Therefore, EHITS_18 has a relatively low NMRScore compared to other poses, but its value is still far from the value of the native structure (see Figure 8). Despite the presence of this alternative conformation, NMRScore ($\rho = 0.55$) is much more correlated with structural RMSD than the EHITS scoring function ($\rho = 0.05$).

FlexX. The poses generated by FlexX are clustered in a small RMSD range from 1.5 Å to 2.2 Å, which is close to the native structure (see Figure 9). Their CSP RMSDs range from 1.3 to 2.3 ppm. FlexX_16 has the best NMRScore with a close-to-native structure (RMSD = 1.6 Å). FlexX_9 has the largest CSP RMSD of 2.3 ppm with a similar structure (RMSD = 1.7 Å). Most of their deviations come from H51 and H52 in the pyrrolidine ring because these two protons in FlexX_9 are in very close proximity to aromatic rings in FKBP, leading to unreasonably large chemical shift perturbations (−3.3 and −10.6 ppm, respectively). Actually all poses from FlexX suffer from this problem, hinting that the nonbonded parameters are too forgiving with respect to close contacts. This results show that NMRScore is exquisitely sensitive to subtle differences of the ligand pose within the binding pocket, which allows us to detect unrealistic close contacts from a set of docking poses.

Fred. We selected the chemgauss2 scoring function implemented in the Fred docking program to score all Fred docking poses. In addition, we were able to score ten NMR structures using this scoring function (see Figure 10A). The chemgauss2 scoring function ranks NMR_6 as the best scoring structure, but mingles the rest of NMR structures with the docking poses. All top-ranked poses docked by Fred are clustered into the RMSD range from 1 Å to 3 Å except Fred_26 (structural RMSD: 4.1 Å). As mentioned before for AutoDock_19, Fred_26 docks the pyridine ring into a shallow groove formed by Phe46, Phe48, and Glu54, while keeping other structural features close to the NMR structure. Consequently, the CSP RMSD of Fred_26 is quite low (0.42 ppm). Many other docked poses with low structural RMSD also have better NMRScores, some even better than several of the NMR structures (see Figure 10B). NMRScore also top-ranks the pose with the lowest structural RMSD. We conclude that while Fred is able to

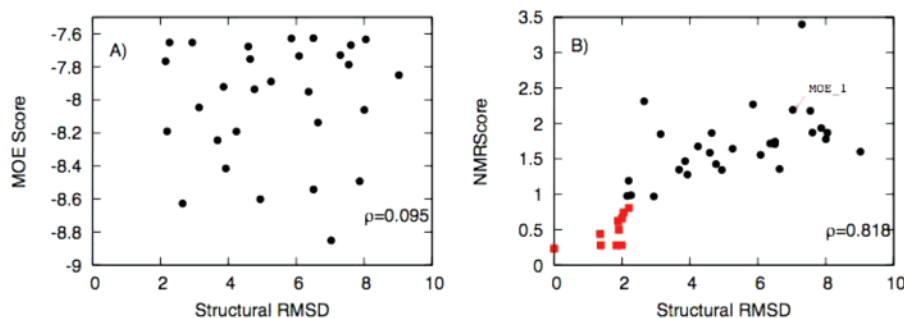


Figure 15. (A) MOE Score vs the structural RMSD. (B) NMRScore *versus* the structural RMSD using MOE poses. The red squares represent the experimental NMR ensemble structures of the GPI-FKBP complex.

generate many correct native-like structures, its chemgauss2 scoring function ranks them inconsistently with structural RMSD ($\rho = 0.08$). However, NMRScore gives an improved ranking according to structural RMSD ($\rho = 0.58$). Overall, FRED generated many relevant poses, but its score function produced more of a scatter, which is partially alleviated by applying NMRScore.

Glide. The structures docked by Glide cover a structural RMSD range from 0.6 Å to 7.4 Å, which were clustered into four groups (see Figure 11). The first group includes the poses with RMSD values from 0.6 Å to 2 Å, which have native-like structures. They are generally highly ranked according to the Glide scoring function (more negative) and NMRScore (lower CSP RMSD). The poses in the second group dock the isopentyl group deep into the major binding pocket, which gives a relatively large RMSD around 4–5 Å. Some of these structures are ranked high by Glide Score (see Figure 11A), but usually have a poor NMRScores (see Figure 11B). For example, Glide_5 belongs to this group and has an NMRScore of 1.9 ppm. The structures in the third group are just like Dock_3, Dock_6, and EHITS_18 described above: the isopentyl and pyridine parts switch their positions while the pyrrolidine ring is locked into the central binding site (RMSD ~ 6 –7). Therefore, these structures have a good NMRScore even though their RMSD from the native pose is quite large. There are three poses, Glide_18, Glide_19, and Glide_22, in the last group, which have a structural RMSD over 7 Å because the pyridine ring of these structures lies in the major binding pocket. All of these structures are ranked poorly based upon both Glide Score and NMRScore.

LibDock. The structural RMSDs for LibDock poses range from 1.6 Å to 4.4 Å. LibDock_1 has an NMRScore of 1.19 ppm with 2 Å RMSD from the native structure. However, there are many poses with similar structures that were poorly ranked (more positive) according to the LibDock scoring function (see Figure 12A). Therefore, the LibDock scoring function cannot tell which native-like pose is the most favorable ($\rho = 0.36$). Interestingly, LibDock_28 (see Figure 13) has the best NMRScore (CSP RMSD = 0.68 ppm) with 2.5 Å RMSD from the native structure (see Figure 12B). The isopentyl part of this pose is quite different from the native structure, but the pyrrolidine ring retains its position. Therefore, most of its CSP RMSD originates from the positioning of the isopentyl protons. LibDock_29 shares the same feature. The Spearman correlation coefficient for NMRScore is 0.62, which indicates it significantly correlated with structural RMSD.

MOE. The top 30 ranked poses span a structural RMSD from 2 Å to 9 Å. The isopentyl moiety in the highest ranked pose (MOE_1) docks deep into the central hydrophobic binding pocket (see Figure 14), resulting in a very large structural RMSD (7.0 Å) with one of the worst NMRScores (CSP RMSD = 2.2 ppm). As shown in Figure 15A, the MOE scoring function

cannot differentiate the close-to-native structures from the far-from-native structures ($\rho = 0.1$). However, based on NMRScore, the closer to the native structure the docking pose (the smaller structural RMSD), the lower CSP RMSD (see Figure 15B). Therefore, NMRScore is better than MOE in scoring and identifying native-like docking poses ($\rho = 0.82$).

Conclusions

We have compared NMRScore with several “traditional” scoring functions associated with popular docking programs using the FKBP–GPI complex as our model system. Generally, these docking programs were able to find the correct binding site, but overall they were unable to differentiate native-like poses from non-native for this system. By incorporating some easily measured NMR experimental data (such as CSP), NMRScore can clearly differentiate native from non-native poses. FlexX generates native-like structures but puts the ligand very close to the protein, as detected by NMRScore. Fred had the best docking structures, which have the lowest CSP RMSD and structural RMSD from the NMR structure. NMRScore, in conjunction with a docking program, can be used to determine the ligand orientation inside a protein binding pocket. For some poses (Dock_3, Dock_6, EHITS_18), the isopentyl group and pyridine ring switch their positions, leading to false positives for NMRScore. This “ligand orientation problem” can be corrected through the inclusion of CSPs from protein residues or experimental NOE information, which is the subject of future studies. The utilization of the STD NMR experiment⁸ also can eliminate this problem. This study represents only one protein–ligand complex system with proton CSPs, but work is underway to extend this procedure to other complexes with other nuclei such as ¹³C, ¹⁵N, ¹⁹F, in order to further validate NMRScore. Nonetheless, we conclude that NMRScore, which incorporates experimental NMR CSP information, is better than other energy-based scoring functions in terms of scoring native-like protein–ligand complexes.

Acknowledgment. We thank the NIH for an STTR grant (GM075636) and the NSF (MCB-0211639) for financial support. We would like to thank Dr. Charles Reynolds (Johnson and Johnson) for the Glide results, Dr. David Diller (Pharmacoceia, Inc.) for the LibDock results, Dr. Alex Clark (Chemical Computing Group) for the MOE results, and Dr. Peter Oledzki (BioSolveIT GmbH) for the FlexX results. We also thank the OpenEye for access to FRED and SimBioSys, Inc. for access to eHiTS.

References

- Brooijmans, N.; Kuntz, I. D. Molecular recognition and docking algorithms. *Annu. Rev. Biophys. Biomol. Struct.* **2003**, *32*, 335–73.
- Alvarez, J. C. High-throughput docking as a source of novel drug leads. *Curr. Opin. Chem. Biol.* **2004**, *8* (4), 365–70.

- (3) Kitchen, D. B.; Decornez, H.; Furr, J. R.; Bajorath, J. Docking and scoring in virtual screening for drug discovery: methods and applications. *Nat. Rev. Drug Discovery* **2004**, *3* (11), 935–49.
- (4) Shoichet, B. K. Virtual screening of chemical libraries. *Nature* **2004**, *432* (7019), 862–5.
- (5) Mohan, V.; Gibbs, A. C.; Cummings, M. D.; Jaeger, E. P.; DesJarlais, R. L. Docking: successes and challenges. *Curr. Pharm. Des.* **2005**, *11* (3), 323–33.
- (6) Hajduk, P. J.; Mack, J. C.; Olejniczak, E. T.; Park, C.; Dandliker, P. J.; Beutel, B. A. SOS-NMR: A saturation transfer NMR-based method for determining the structures of protein-ligand complexes. *J. Am. Chem. Soc.* **2004**, *126* (8), 2390–2398.
- (7) Constantine, K. L.; Davis, M. E.; Metzler, W. J.; Mueller, L.; Claus, B. L. Protein-ligand NOE matching: a high-throughput method for binding pose evaluation that does not require protein NMR resonance assignments. *J. Am. Chem. Soc.* **2006**, *128* (22), 7252–63.
- (8) Mayer, M.; Meyer, B. Characterization of ligand binding by saturation transfer difference NMR spectroscopy. *Angew. Chem., Int. Ed.* **1999**, *38* (12), 1784–1788.
- (9) Kollman, P., Free-Energy Calculations - Applications to Chemical and Biochemical Phenomena. *Chem. Rev.* **1993**, *93* (7), 2395–2417.
- (10) Lamb, M. L.; Jorgensen, W. L. Computational approaches to molecular recognition. *Curr. Opin. Chem. Biol.* **1997**, *1* (4), 449–57.
- (11) Gohlke, H.; Klebe, G. Approaches to the description and prediction of the binding affinity of small-molecule ligands to macromolecular receptors. *Angew. Chem., Int. Ed.* **2002**, *41* (15), 2645–2676.
- (12) Simonson, T.; Archontis, G.; Karplus, M. Free energy simulations come of age: protein-ligand recognition. *Acc. Chem. Res.* **2002**, *35* (6), 430–7.
- (13) Morris, G. M.; Goodsell, D. S.; Halliday, R. S.; Huey, R.; Hart, W. E.; Belew, R. K.; Olson, A. J. Automated docking using a Lamarckian genetic algorithm and an empirical binding free energy function. *J. Comput. Chem.* **1998**, *19* (14), 1639–1662.
- (14) Ewing, T. J.; Makino, S.; Skillman, A. G.; Kuntz, I. D. DOCK 4.0: search strategies for automated molecular docking of flexible molecule databases. *J. Comput.-Aided Mol. Des.* **2001**, *15* (5), 411–28.
- (15) Eldridge, M. D.; Murray, C. W.; Auton, T. R.; Paolini, G. V.; Mee, R. P. Empirical scoring functions: I. The development of a fast empirical scoring function to estimate the binding affinity of ligands in receptor complexes. *J. Comput.-Aided Mol. Des.* **1997**, *11* (5), 425–45.
- (16) Bohm, H. J. Prediction of binding constants of protein ligands: a fast method for the prioritization of hits obtained from de novo design or 3D database search programs. *J. Comput.-Aided Mol. Des.* **1998**, *12* (4), 309–23.
- (17) Wang, R.; Lai, L.; Wang, S. Further development and validation of empirical scoring functions for structure-based binding affinity prediction. *J. Comput.-Aided Mol. Des.* **2002**, *16* (1), 11–26.
- (18) Muegge, I.; Martin, Y. C. A general and fast scoring function for protein-ligand interactions: a simplified potential approach. *J. Med. Chem.* **1999**, *42* (5), 791–804.
- (19) Gohlke, H.; Hendlich, M.; Klebe, G. Knowledge-based scoring function to predict protein-ligand interactions. *J. Mol. Biol.* **2000**, *295* (2), 337–56.
- (20) Bissantz, C.; Folkers, G.; Rognan, D. Protein-based virtual screening of chemical databases. 1. Evaluation of different docking/scoring combinations. *J. Med. Chem.* **2000**, *43* (25), 4759–67.
- (21) Stahl, M.; Rarey, M. Detailed analysis of scoring functions for virtual screening. *J. Med. Chem.* **2001**, *44* (7), 1035–42.
- (22) Wang, R.; Lu, Y.; Wang, S. Comparative evaluation of 11 scoring functions for molecular docking. *J. Med. Chem.* **2003**, *46* (12), 2287–303.
- (23) Warren, G. L.; Andrews, C. W.; Capelli, A. M.; Clarke, B.; LaLonde, J.; Lambert, M. H.; Lindvall, M.; Nevins, N.; Semus, S. F.; Senger, S.; Tedesco, G.; Wall, I. D.; Woolven, J. M.; Peishoff, C. E.; Head, M. S. A critical assessment of docking programs and scoring functions. *J. Med. Chem.* **2006**, *49* (20), 5912–31.
- (24) Abagyan, R.; Totrov, M. High-throughput docking for lead generation. *Curr. Opin. Chem. Biol.* **2001**, *5* (4), 375–82.
- (25) Wang, B.; Brothers, E. N.; Van Der Vaart, A.; Merz, K. M. Fast semiempirical calculations for nuclear magnetic resonance chemical shifts: A divide-and-conquer approach. *J. Chem. Phys.* **2004**, *120* (24), 11392–400.
- (26) Wang, B.; Raha, K.; Merz, K. M. Pose Scoring by NMR. *J. Am. Chem. Soc.* **2004**, *126*, 11430–11431.
- (27) Sich, C.; Improt, S.; Cowley, D. J.; Guenet, C.; Merly, J. P.; Teufel, M.; Saudek, V. Solution structure of a neurotrophic ligand bound to FKBP12 and its effects on protein dynamics. *Eur. J. Biochem.* **2000**, *267* (17), 5342–5354.
- (28) Zsoldos, Z.; Reid, D.; Simon, A.; Sadjad, B. S.; Johnson, A. P. eHiTS: an innovative approach to the docking and scoring function problems. *Curr. Protein Pept. Sci.* **2006**, *7* (5), 421–35.
- (29) Rarey, M.; Kramer, B.; Lengauer, T.; Klebe, G. A fast flexible docking method using an incremental construction algorithm. *J. Mol. Biol.* **1996**, *261* (3), 470–489.
- (30) McGann, M. R.; Almond, H. R.; Nicholls, A.; Grant, J. A.; Brown, F. K. Gaussian docking functions. *Biopolymers* **2003**, *68* (1), 76–90.
- (31) Friesner, R. A.; Banks, J. L.; Murphy, R. B.; Halgren, T. A.; Klicic, J. J.; Mainz, D. T.; Repasky, M. P.; Knoll, E. H.; Shelley, M.; Perry, J. K.; Shaw, D. E.; Francis, P.; Shenkin, P. S. Glide: a new approach for rapid, accurate docking and scoring. 1. Method and assessment of docking accuracy. *J. Med. Chem.* **2004**, *47* (7), 1739–49.
- (32) Halgren, T. A.; Murphy, R. B.; Friesner, R. A.; Beard, H. S.; Frye, L. L.; Pollard, W. T.; Banks, J. L. Glide: a new approach for rapid, accurate docking and scoring. 2. Enrichment factors in database screening. *J. Med. Chem.* **2004**, *47* (7), 1750–9.
- (33) Diller, D. J.; Merz, K. M., Jr., High throughput docking for library design and library prioritization. *Proteins* **2001**, *43* (2), 113–24.
- (34) Diller, D. J.; Li, R., Kinases, homology models, and high throughput docking. *J. Med. Chem.* **2003**, *46* (22), 4638–47.
- (35) Chemical Computing Group, C. C. *MOE 2006.08*, Montreal, Quebec, Canada H3A 2R7, 2006.
- (36) Case, D. A.; Cheatham, T. E., III; Darden, T.; Gohlke, H.; Luo, R.; Merz, K. M., Jr.; Onufriev, A.; Simmerling, C.; Wang, B.; Woods, R. J. The Amber biomolecular simulation programs. *J. Comput. Chem.* **2005**, *26* (16), 1668–88.
- (37) Cornell, W. D.; Cieplak, P.; Bayly, C. I.; Gould, I. R.; Merz, K. M.; Ferguson, D. M.; Spellmeyer, D. C.; Fox, T.; Caldwell, J. W.; Kollman, P. a., A 2nd Generation Force-Field for the Simulation of Proteins, Nucleic-Acids, and Organic-Molecules. *J. Am. Chem. Soc.* **1995**, *117* (19), 5179–5197.
- (38) Wang, B.; Raha, K.; Liao, N.; Peters, M. B.; Kim, H.; Westerhoff, L. M.; Wollacott, A. M.; van de Vaart, A.; Gogonea, V.; Suarez, D.; Dixon, S. L.; Vincent, J. J.; Brothers, E. N.; Merz, K. M. DivCon, 2005.

JM070484A